Journal of Medicinal Chemistry

Article

pubs.acs.org/jmc

Toward the Definition of Stereochemical Requirements for MT_2-Selective Antagonists and Partial Agonists by Studying 4-Phenyl-2-propionamidotetralin Derivatives

Annalida Bedini,[†] Simone Lucarini,[†] Gilberto Spadoni,[†] Giorgio Tarzia,[†] Francesco Scaglione,[‡] Silvana Dugnani,[‡] Marilou Pannacci,[‡] Valeria Lucini,[‡] Caterina Carmi,[§] Daniele Pala,[§] Silvia Rivara,*[,§] and Marco Mor[§]

[†]Dipartimento di Scienze Biomolecolari, Università degli Studi di Urbino "Carlo Bo", Piazza Rinascimento 6, I-61029 Urbino, Italy

[‡]Dipartimento di Farmacologia, Chemioterapia e Tossicologia Medica, Università degli Studi di Milano, Via Vanvitelli 32, I-20129 Milano, Italy

[§]Dipartimento Farmaceutico, Università degli Studi di Parma, Viale G. P. Usberti 27/A Campus Universitario, I-43124 Parma, Italy

Supporting Information

ABSTRACT: New derivatives of 4-phenyl-2-propionamidotetralin (4-P-PDOT) were prepared and tested on cloned MT_1 and MT_2 receptors, with the purpose of merging previously reported pharmacophores for nonselective agonists and for MT_2-selective antagonists. A 8-methoxy group increases binding affinity of both (±)-*cis*- and (±)-*trans*-4-P-PDOT, and it can be bioisosterically replaced by a bromine. Conformational analysis of 8-methoxy-4-P-PDOT by molecular dynamics, supported by NMR data, revealed an energetically favored conformation for the (2*S*,4*S*)-*cis* isomer and a less favorable conformation for the (2*R*,4*S*)-*trans* one, fulfilling the requirements of a pharmacophore model for nonselective melatonin receptor agonists. A new superposition model, including features characteristic of MT_2-selective antagonists, suggests that MT_1/MT_2 agonists and MT_2 antagonists can share the same arrangement for their pharmacophoric elements. The model correctly predicted the eutomers of (±)-*cis*- and (±)-*trans*-4-P-PDOT. The model was validated by preparing three dihydronaphthalene derivatives, either able or not able to reproduce the putative active conformation of 4-P-PDOT.

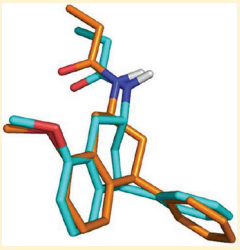

INTRODUCTION

Melatonin (Figure 1) is a tryptophan-derived hormone secreted by the pineal gland following a circadian rhythm, with peak levels occurring during the period of darkness. Besides its well-known chronobiotic and sleep-inducing properties,[1] many other effects have been ascribed to melatonin, such as the modulation of cardiovascular[2] and immune systems,[3] bone formation,[4] and hormone secretion.[5] For this reason melatonin has been proposed as a therapeutic agent in a variety of pathological conditions, such as sleep disturbances,[6] cancer,[7] neurodegenerative diseases,[8] and stroke.[9] Melatonin binds to and activates two G-protein-coupled receptors, MT_1 and MT_2, mainly expressed in the central nervous system but also present in peripheral organs.[10,11] Moreover, an additional melatonin binding site, named *MT*$_3$, has been reported as the hamster homologue of the human enzyme quinone reductase 2, which is thought to be involved in melatonin-mediated antioxidant activity.[12]

The past decade has brought significant advancements in the design and development of MT_1 and MT_2 receptor ligands, as well as in their therapeutic application. Melatonin, in a prolonged-release formulation,[13] and ramelteon[14] (Figure 1) are prescribed for the treatment of insomnia; agomelatine[15] (Figure 1), an MT_1/MT_2 agonist and $5HT_{2C}$ antagonist, has been approved for the treatment of major depressive disorders, and other agonists are currently being tested in clinical trials.[16] Besides nonselective ligands, different series of MT_1- or MT_2-selective agents have also been described.[17−19] Investigations on the role of melatonin receptors depend on the availability of potent and selective ligands. The MT_2-selective antagonist/partial agonist 4-phenyl-2-propionamidotetralin[20] (4-P-PDOT, Figure 1), together with luzindole,[20] played a key role as a pharmacological tool for the evaluation of specific effects of melatonin and melatonin receptor ligands. In particular, 4-P-PDOT has been widely employed to discriminate the role of MT_1 and MT_2 receptors in melatonin-mediated effects. 4-P-PDOT revealed 100-fold selectivity for the MT_2 receptor and antagonist behavior on electrically evoked dopamine release in rabbit retina.[20] However, it showed different degrees of intrinsic activity in different experiments; e.g., it behaved as an MT_1 antagonist/MT_2 partial agonist in tests based on GTPγS binding or cAMP formation.[21−23] Because of its two asymmetric carbons, there are two couples of 4-P-PDOT enantiomers, corresponding to the *cis* and *trans* isomers. In many cases, the use of 4-P-PDOT had been reported without clear indications about composition of the mixture employed.

Received: June 17, 2011
Published: November 2, 2011

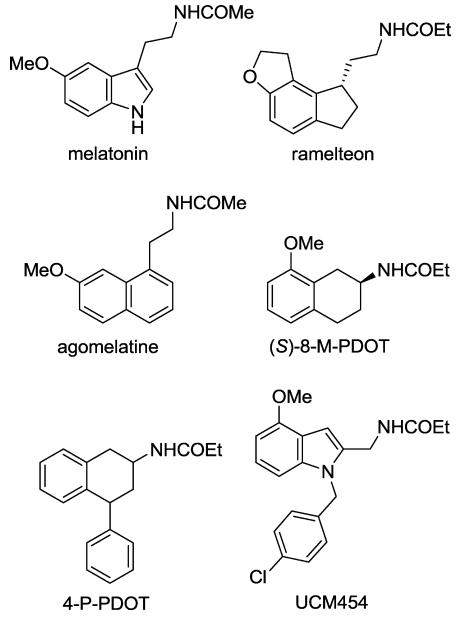

Figure 1. Melatonin and selected melatonin receptor ligands.

In spite of the importance of 4-P-PDOT, structure−activity relationships (SARs) for 4-phenyl-2-acylaminotetralin derivatives have been poorly explored. Only two analogues of 4-P-PDOT, characterized by minor modifications at the acylating group, have been described in the literature, showing that both the *N*-acetyl and *N*-chloroacetyl derivatives have binding affinities similar to that of 4-P-PDOT.[20] Furthermore it was reported that (±)-*cis*-4-P-PDOT displays higher MT_2 binding affinity than the (±)-*trans*-isomer and that both racemic mixtures showed selectivity for the MT_2 receptor.[24] No information about the role of a key element for the pharmacophore of melatonin receptor ligands, i.e., the 5-methoxy group of melatonin, had been reported so far. Moreover, while the structure of 4-P-PDOT can be easily superposed to the putative active conformations of other MT_2-selective antagonists,[25] the relevance of amide group orientation, with respect to the lipophilic portions, has not been assessed so far.

The aim of this work is to focus on the active conformation and configuration of 4-P-PDOT derivatives, to test the hypothesis that it is possible to merge a pharmacophore model for melatonin receptor agonists[26] and one for MT_2-selective antagonists.[25,27] These models share an aromatic nucleus and an amide fragment, whereas a lipophilic group with an out-of plane arrangement is typical for MT_2-selective antagonists. While the MT_2-antagonists pharmacophore model led to the design of new MT_2-selective ligands,[28,29] it contains no information about stereoselectivity or about the conformation of the alkylamide side chain. On the other hand, the pharmacophore model for nonselective melatonin receptor agonists[26] accounted for stereoselectivity and side chain conformation. Starting from the observed stereoselectivity for the two enantiomers of a conformationally constrained tricyclic melatonin analogue, it had been observed that a putative active conformation of melatonin, having the acetylaminoethyl chain below the plane of indole ring (as represented in Figure 1), could be efficiently superposed to the eutomers of stereoselective agonists. In spite of the conformational constraint in the tricyclic structure, however, the acetylamino group was free to rotate, and the active orientation of this pharmacophore element was therefore ill-defined. Furthermore, no evidence has been presented so far that the common pharmacophore elements have the same mutual arrangement for both the "agonist" and the "MT_2-selective antagonist" binding modes.

The purpose of the present work is to develop a unique superposition model for both classes of ligands, based on stereoselectivity data for 4-P-PDOT derivatives. Such a model could be useful not only to drive the development of new classes of ligands with tailored subtype selectivity and/or intrinsic activity but also to select the bioactive conformation of MT_2-selective ligands that can be used to refine MT_2 receptor models built by homology modeling. We therefore prepared 8-methoxy derivatives of both *cis*- and *trans*-4-P-PDOT and the corresponding bromine bioisoster for the more potent racemate. Once assessed that the role of these groups was the same as observed in known classes of agonists, we explored the accessible conformational space of the two diastereomers by stochastic dynamics simulations and NMR. A superposition of energetically accessible conformations, consistent with both cited pharmacophore models, also was consistent with the affinity ratios for pure (2*S*,4*S*)-, (2*R*,4*S*)-, (2*R*,4*R*)-, and (2*S*,4*R*)-4-P-PDOT, which had been recently separated and characterized.[30] The superposition model was further validated by preparing dihydronaphthalene analogues that either could or could not be closely superposed to the putative active conformation of 4-P-PDOT.

RESULTS AND DISCUSSION

Synthesis of 4-P-PDOT Derivatives. Compounds **3a,b** and **4b,c** were prepared in a reaction sequence already employed by our group[31] for the synthesis of *cis*-4-P-PDOT (Scheme 1), involving condensation of the suitable tetralone **2a−c** with propionamide in the presence of PTSA and azeotropic removal of water, followed by ionic diastereoselective reduction (Et_3SiH/TFA) of the cyclic enamides **3a−c**. The key tetralones **2a−c** were obtained by reaction of styrene with the appropriate phenylacetyl chloride **1a−c** in the presence of aluminum chloride.

Target compound **6** was synthesized by a four-step procedure starting from the tetralone **2a**.[31] As shown in Scheme 1, the first step involved the reaction of **2a** with trimethylsilyl cyanide and ZnI_2 followed by treatment with phosphorus oxychloride in pyridine to give the intermediate nitrile **5** which was converted into the final product **6** by reduction with $LiAlH_4$ and acylation of the intermediate amine with propionic anhydride.

Starting from the tetralone **2b** the (±)-*trans*-propionamidotetralin derivative **10** was prepared in a reaction sequence already applied for similar compounds,[32] involving a diastereoselective (85:15 *cis*/*trans*) ketone reduction using $NaBH_4$, followed by tosylation of the resulting 2-tetralol **7** with *p*-toluensulfonyl chloride in pyridine. The *cis*-tosylate **8** was then converted to the corresponding (±)-*trans*-propionamido derivative **10** by reaction with sodium azide in aqueous DMF, followed by catalytic (10% Pd/C) hydrogenation and acylation of the intermediate amine with propionic anhydride (Scheme 2).

Pharmacological Characterization of 8-Substituted 4-P-PDOT Derivatives. Binding affinity and intrinsic activity at human MT_1 and MT_2 receptors for newly synthesized compounds and for recently separated four 4-P-PDOT single stereoisomers are reported in Tables 1 and 2. To improve data homogeneity for SAR comparisons, the racemic mixtures (±)-*cis*- and (±)-*trans*-4-P-PDOT were tested during the experimental runs carried out for new compounds. The introduction of a methoxy group in position

dx.doi.org/10.1021/jm200790v | *J. Med. Chem.* 2011, 54, 8362−8372

Scheme 1[a]

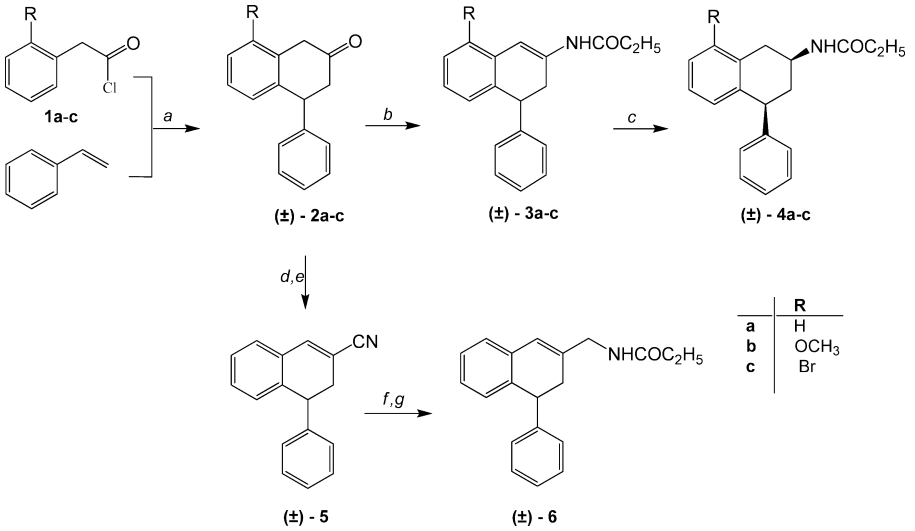

[a]Reagents and conditions: (a) $AlCl_3$, CH_2Cl_2, 0 °C, 15 min; (b) propionamide, PTSA, toluene, reflux, 4 h; (c) TES, TFA, −10 °C, 10 min; (d) $(CH_3)_3SiCN$, ZnI_2, toluene, room temp, 18 h; (e) $POCl_3$, Py, reflux, 1 h; (f) $LiAlH_4$, Et_2O, room temp, 15 min; (g) propionic anhydride, TEA, THF, room temp, 16 h.

Scheme 2[a]

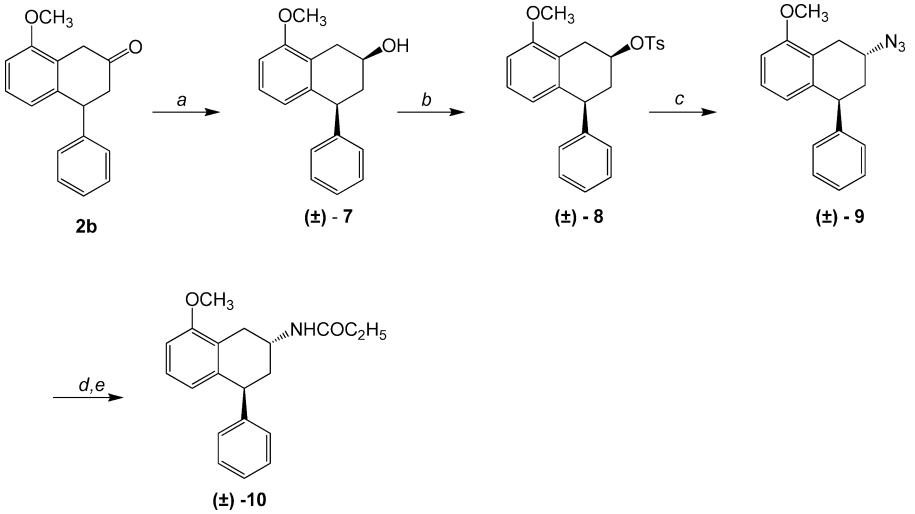

[a]Reagents and conditions: (a) $NaBH_4$, MeOH, reflux, 16 h; (b) TsCl, Py, 5 °C, 3 days; (c) NaN_3, DMF/H_2O, 50 °C, 5 h; (d) H_2 (4 atm), 10% Pd/C, *i*-PrOH/CH_2Cl_2, room temp, 16 h; (e) propionic anhydride, TEA, THF, room temp, 4 h.

8 caused a moderate increase of MT_1 and MT_2 binding affinity for both the *cis* and *trans* racemic mixtures of 4-P-PDOT derivatives (compounds **4b** and **10**), consistent with what had been observed for a series of 2-propionamidotetralins, including the agonist 8-M-PDOT (Figure 1).[33] The racemic mixtures **4b** and **10** showed low to medium intrinsic activity at the GTPγS test, with no increase of intrinsic activity compared to the respective 4-P-PDOT racemates. The affinity ratio between *cis* and *trans* racemates was fully conserved, as well as selectivity for receptor subtypes. Thus, the positive effect of the 8-methoxy group on binding affinity resembles what had been observed in other series of melatonin receptor ligands.[25,28,29,34−38] Replacement of the 8-methoxy group of the better racemate, **4b**, by a bromine atom gave **4c**, showing MT_1 and MT_2 affinities comparable to, or slightly better than, those of the methoxy derivative **4b** and a moderate increase of intrinsic activity. This is consistent with what had been previously observed for other series of melatonin ligands, e.g., in the series of melatonin derivatives[39] and of *N*-anilinoethylamides.[29]

NMR Analysis and SD Simulations on *cis*- (4b) and *trans*-8-Methoxy-4-P-PDOT (10). The observation that 4-P-PDOT derivatives show SAR patterns (constant effect of the 8-methoxy group, bioisosterism with bromine) matching those of typical melatonin receptor agonists prompted us to apply a chiral pharmacophore model, previously developed for stereoselective, MT_1/MT_2 nonselective agonists,[26] to the search for active conformations of 4-P-PDOT stereoisomers. In previous work, it had been observed that conformational equilibrium of the tetralin nucleus can qualitatively explain the different affinity for *cis* and *trans* isomers, but no experimental data on single stereoisomers were available, and, regarding conformational aspects, the role of amide orientation was not addressed.[24]

dx.doi.org/10.1021/jm200790v | J. Med. Chem. 2011, 54, 8362−8372

Table 1. Binding Affinity and Intrinsic Activity of Newly Synthesized Compounds 4b,c, 10, and of 4-P-PDOT Stereoisomers for Human MT_1 and MT_2 Melatonin Receptors

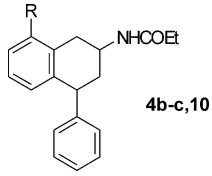

4b-c,10

			MT_1		MT_2	
compd	R	stereochemistry	$pK_i \pm SEM^a$	$IAr \pm SEM^b$	$pK_i \pm SEM^a$	$IAr \pm SEM^b$
melatonin			9.58 ± 0.15	1.00 ± 0.05	9.47 ± 0.12	1.00 ± 0.03
4b	OCH_3	(±)-*cis*	7.83 ± 0.07	0.20 ± 0.02	10.22 ± 0.38	0.44 ± 0.07
10	OCH_3	(±)-*trans*	7.04 ± 0.06	0.02 ± 0.01	9.71 ± 0.42	0.21 ± 0.03
4c	Br	(±)-*cis*	7.99 ± 0.16	0.49 ± 0.08	10.85 ± 0.20	0.65 ± 0.09
(±)-*cis*-4-P-PDOT[c]	H	(±)-*cis*	7.12 ± 0.22	0.23 ± 0.06	9.16 ± 0.06	0.46 ± 0.02
(±)-*trans*-4-P-PDOT[c]	H	(±)-*trans*	6.65 ± 0.07	0.41 ± 0.07	8.06 ± 0.08	0.40 ± 0.01
(2*S*,4*S*)-4-P-PDOT[d]	H	(+)-*cis*	7.02 ± 0.11	0.15 ± 0.08	9.26 ± 0.14	0.45 ± 0.01
(2*R*,4*R*)-4-P-PDOT[d]	H	(−)-*cis*	6.59 ± 0.06	0.06 ± 0.02	7.01 ± 0.05	0.11 ± 0.02
(2*R*,4*S*)-4-P-PDOT[d]	H	(+)-*trans*	6.89 ± 0.09	0.33 ± 0.04	8.02 ± 0.15	0.48 ± 0.05
(2*S*,4*R*)-4-P-PDOT[d]	H	(−)-*trans*	5.67 ± 0.19	−0.23 ± 0.03	6.10 ± 0.15	−0.14 ± 0.04

[a] pK_i values were calculated from IC_{50} values, obtained from competition curves by the method of Cheng and Prusoff,[45] and are the mean of at least three determinations performed in duplicate. [b] The relative intrinsic activity values were obtained by dividing the maximum analogue-induced G-protein activation by that of melatonin. [c] See ref 24. [d] See ref 30.

Table 2. Binding Affinity and Intrinsic Activity of Newly Synthesized Compounds 3a,b and 6 for Human MT_1 and MT_2 Melatonin Receptors

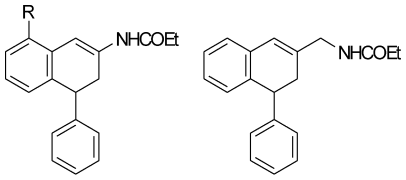

3a-b 6

		MT_1		MT_2	
compd	R	$pK_i \pm SEM^a$	$IA_r \pm SEM^b$	$pK_i \pm SEM^a$	$IA_r \pm SEM^b$
melatonin		9.58 ± 0.15	1.00 ± 0.05	9.47 ± 0.12	1.00 ± 0.03
(±)-**3a**	H	7.30 ± 0.12	0.14 ± 0.03	7.43 ± 0.31	0.59 ± 0.11
(±)-**3b**	OCH_3	6.74 ± 0.32	0.32 ± 0.06	7.11 ± 0.28	0.49 ± 0.05
(±)-**6**	H	7.69 ± 0.09	0.01 ± 0.06	8.46 ± 0.12	0.02 ± 0.05

[a] pK_i values were calculated from IC_{50} values, obtained from competition curves by the method of Cheng and Prusoff,[45] and are the mean of at least three determinations performed in duplicate. [b] The relative intrinsic activity values were obtained by dividing the maximum analogue-induced G-protein activation by that of melatonin.

To explore the accessible conformations of 4-P-PDOT derivatives, detailed conformational analysis for compounds **4b** and **10** was performed, complementing molecular dynamics simulations with NMR experiments. The *cis* racemic mixture **4b** showed $^1H-^1H$ vicinal coupling constants (^3J, Table 3) for the cyclohexenyl ring consistent with a half-chair conformation, with equatorial amide chain and pseudo-equatorial phenyl ring. 2D NOESY data (Supporting Information, Figure S1) also supported the presence of a single conformation for the tetralin scaffold. In particular, by reference to the structure of **4b** reported in Figure 2, strong NOE cross-peaks were observed between protons H1b and H3b and between H2 and H4, all in pseudoaxial or axial arrangement, while no cross-peak was detected between the equatorial H1a and H3a. Additional NOEs were detected: between the *O*-methyl protons at position 8 and H7; between Ho and H3b, H4 and H5; between NH and H1b, H3b, and the α-CH_2 of the propionamide side chain. NMR spectra of the *trans* isomer **10** are consistent with the presence of two conformations in rapid exchange, similar to what had been observed for *trans*-4-P-PDOT.[24] In fact, $^1H-^1H$ vicinal coupling constants (^3J, Table 3) for the cyclohexene ring showed intermediate values consistent with an equilibrium between two half-chair conformations, one with equatorial amide side chain and pseudoaxial phenyl ring and the other with axial amide and pseudoequatorial phenyl ring. Cross-peaks in the NOESY spectrum (Supporting Information, Figure S2) also supported the presence of a conformational equilibrium. In fact, cross-peaks consistent with both conformations were detected with similar intensities (equatorial amide side chain: between H1a and H3a, between H2 and Ho; axial amide side chain: between H1b and H3b, between H4 and NH). Intense NOEs were also observed between *O*-methyl protons at position 8 and H7; between aromatic Ho and H3a, H4 and H5; and between NH and H1a, H2, H3a, and the propionamidic α-CH_2.

dx.doi.org/10.1021/jm200790v | J. Med. Chem. 2011, 54, 8362–8372

Table 3. Geminal and Vicinal Coupling Constants Values Observed by NMR Spectroscopy (600 MHz) and Calculated for Compounds 4b and 10

		4b, coupling constant (Hz)		**10**, coupling constant (Hz)			
					calcd		
protons[a]	type of coupling	obsd	calcd[b]	obsd	av[b]	ax[c]	eq[c]
H1a-H1b	geminal (^2J)	16.8		17.4			
H3a-H3b	geminal (^2J)	12.0		12.6			
H1b-H2	vicinal (^3J)	10.8	10.7	5.4	4.2	3.8	5.3
H1a-H2	vicinal (^3J)	5.4	4.5	6.0	5.0	2.9	10.3
H3b-H2	vicinal (^3J)	12.0	11.0	3.0	3.0	2.9	3.2
H3a-H2	vicinal (^3J)	2.4	3.1	7.8	5.8	3.8	11.2
H3b-H4	vicinal (^3J)	12.0	11.1	7.2	8.4	11.0	2.0
H3a-H4	vicinal (^3J)	4.8	4.8	6.0	5.2	5.2	5.2
NH-H2	vicinal (^3J)	7.2		7.2			

[a]Refer to Figure 2 for proton numbering scheme. [b]Average values for 50 000 conformations collected from SD (see Experimental Section). [c]Calculated from conformations of **10** having the amide side chain in axial or in equatorial arrangement.

Stochastic dynamics (SD) trajectories of two single enantiomers of **4b** and **10** [(2*S*,4*S*)-**4b** and (2*R*,4*S*)-**10** were employed as reference structures and are represented in Figures 2 and 3] were registered for a simulation time of 1 μs.

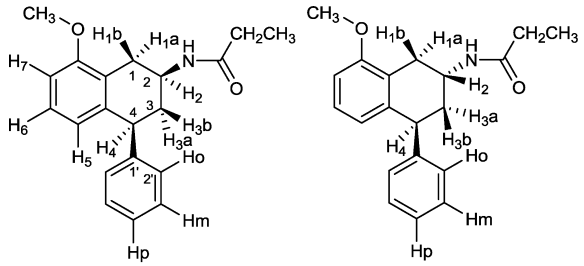

Figure 2. Chemical structures and atom labeling for **4b** and **10**. The (2*S*,4*S*) and the (2*R*,4*S*) enantiomers are reported as representatives of the *cis*-(**4b**) and *trans*-(**10**) racemic mixtures, respectively. Protons below the plane of the tetralin ring are labeled with "a" and those above the plane with "b".

Monitoring the dihedral angle τ_1 (C1−C2−C3−C4, Figure 2), we observed that the half-chair conformation of **4b**, having both substituents in equatorial arrangement (Figure 3, *cis*-**I** and *cis*-**II**), was conserved during the simulation (τ_1 = 60° for (2*S*,4*S*)-**4b**, Figure 4a) and only a small number of snapshots (<2%) presented a conformation with diaxial arrangement (τ_1 = 300° in Figure 4a, *cis*-**III** in Figure 3). (2*R*,4*S*)-**10** underwent repeated conversions between the two cyclohexene conformations characterized by τ_1 = 60° (Figure 4b, *trans*-**I** in Figure 3) and τ_1 = 300° (Figure 4b, *trans*-**II** and *trans*-**III** in Figure 3). The ratio between these two cyclohexene conformations was approximately 30/70, with the more abundant having the 2-propionamido substituent in axial arrangement and the 4-phenyl ring in pseudo-equatorial one. By collection of 50 000 conformations (snapshots) during SD simulation (one every 20 ns) and by represention of cyclohexene arrangements by τ_1 and amide rotamers around the C2−N bond by τ_2 = H2−C2−N−H (Figure 2), the vast majority of snapshots could be grouped in the conformation families reported in Table 4. Considering this set as representative of the dynamic conformational equilibrium (for both **4b** and **10**, more than 200 conversions among different conformation families were observed), we estimated *J* values for vicinal protons as ensemble averages of those calculated from dihedral angles measured for each snapshot. The calculated values are reported in Table 3 and here compared to those experimentally observed. While for **4b** there is good agreement between experimental and theoretical data, some *J* values calculated for **10** were slightly different from experimental ones. In particular, the experimental values of $J_{H3a\text{-}H2}$ and $J_{H3b\text{-}H4}$, which strongly depend on the relative abundance of the two cyclohexene conformations, were 7.8 and 7.2 Hz, respectively, compared to those calculated as averages of SD conformations, being 5.8 and 8.4, respectively. As stated above, SD simulation showed a 30/70 ratio between confromations with the amide chain in equatorial and axial arrangements. In fact, the best agreement between experimental and calculated *J* values for **10** corresponds to a ratio of 45/55, giving $J_{calc,H3a\text{-}H2}$ = 7.1 and $J_{calc,H3b\text{-}H4}$ = 6.9. Although significant, this discrepancy corresponds to limited differences in free energies and does not affect the following superposition hypothesis. The 8-methoxy group mostly assumed one preferred orientation, with the methyl group pointing toward H7 (Supporting Information, Figure S3). This is consistent with the presence of strong NOE signals between methyl

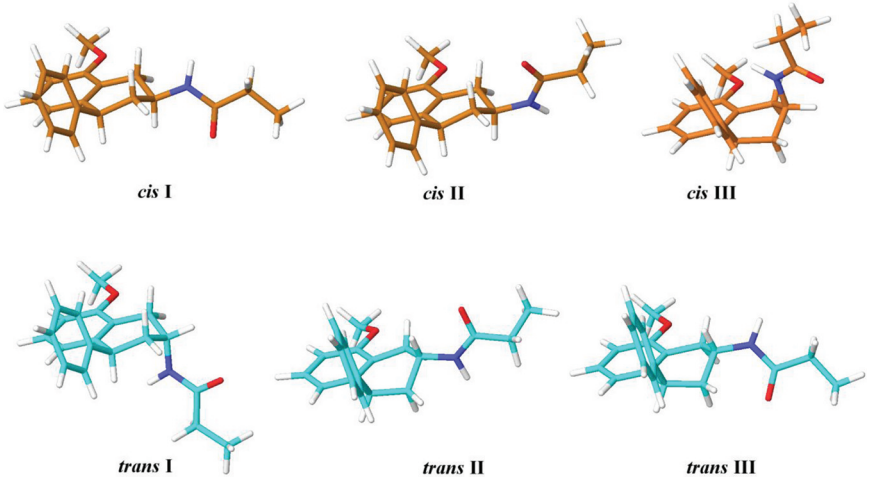

Figure 3. Representation of minimum-energy conformations of (2*S*,4*S*)-**4b** (*cis*) and (2*R*,4*S*)-**10** (*trans*), explored during SD simulations.

dx.doi.org/10.1021/jm200790v | *J. Med. Chem.* 2011, 54, 8362–8372

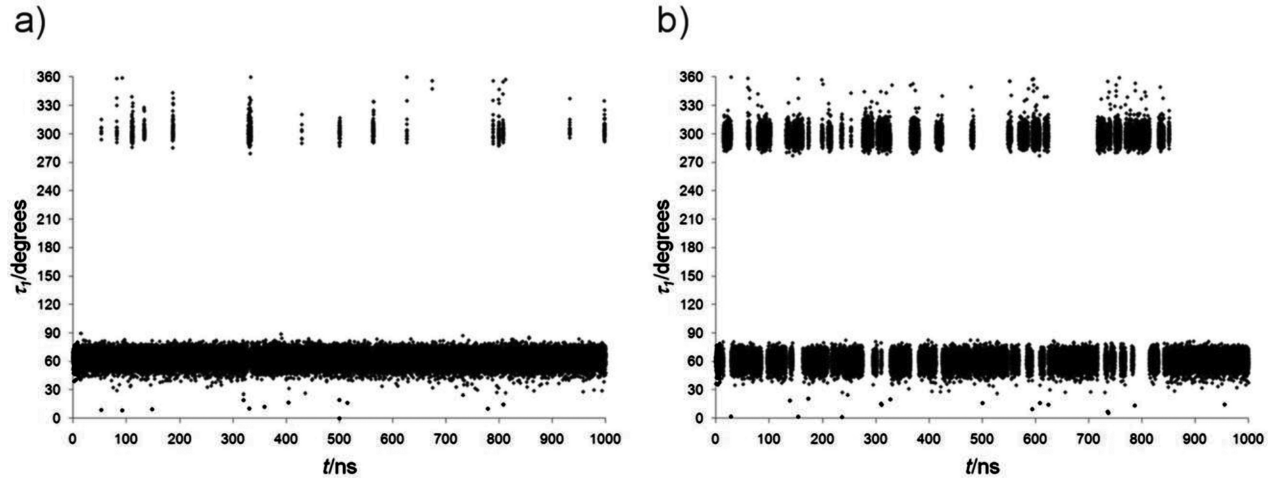

Figure 4. Graphical representation of τ_1 (C1−C2−C3−C4) dihedral angle values for *cis*-(2*S*,4*S*)-**4b** (a) and *trans*-(2*R*,4*S*)-**10** (b).

Table 4. Families of Conformations and Their % Abundance in a Set of 50 000 Snapshots Collected during SD Simulations for Compounds 4b and 10

		range of dihedral angle (deg)		
compd	conformation[a]	τ_1 [b]	τ_2 [b]	%
(2*S*,4*S*)-**4b**				
	cis-**I**	30−90	120−240	96.29
	cis-**II**	30−90	330−360 and 0−60	1.04
	cis-**III**	270−330	120−240	1.59
(2*R*,4*S*)-**10**				
	trans-**I**	30−90	120−240	70.60
	trans-**II**	270−330	120−240	26.72
	trans-**III**	270−330	285−360 and 0−15	0.45

[a]Corresponding to the minimum-energy conformations represented in Figure 3. [b]τ_1 = C1−C2−C3−C4. τ_2 = H2−C2−N−H. See Figure 2 for atom numbering.

protons and H7. The amide NH group was oriented *anti* to H2 during most of the simulation time (>99%) for both **4b** and **10**, with a small number of snapshots presenting an opposite orientation (Supporting Information, Figure S4). On the other hand, both the coupling constant H2−NH (7.2 Hz) and the absence of strong NOE signals between NH and tetralin protons are more consistent with free rotation around the C2−N bond.

Therefore, combined information from NMR data and SD simulations pointed to (i) a preferred diequatorial arrangement of substituents in 2 and 4 for the *cis* isomer **4b**; (ii) an equilibrium, with no overwhelming abundance, between the two half-chair conformations for the *trans* isomer **10**; (iii) a prevalent *anti* orientation of the H2−C2−N−H dihedral, with possible rotation, for both isomers.

Superposition of 8-Methoxy-4-P-PDOT Stereoisomers on Melatonin Active Conformation. The most abundant conformer of **4b**, resulting from SD simulation, could be superposed on the active conformation of melatonin which had been inferred from a pharmacophore model based on stereoselective MT_1/MT_2 agonists, including (*S*)-8-M-PDOT (Figure 5a).[26] The 4-phenyl ring of **4b** represents an element, not present in the agonist pharmacophore, related to MT_2-selectivity and reduced intrinsic activity.[40] When the same conformer of **4b** was superimposed to the MT_2-selective antagonist UCM454, a strict superposition of the amide

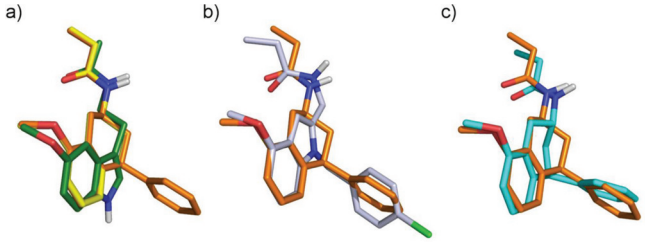

Figure 5. Superposition of (a) melatonin (green carbons), (*S*)-8-M-PDOT (yellow carbons), and *cis*-(2*S*,4*S*)-**4b** (orange carbons); (b) *cis*-(2*S*,4*S*)-**4b** (orange carbons) and UCM454 (white carbons); (c) *cis*-(2*S*,4*S*)-**4b** (orange carbons) and *trans*-(2*R*,4*S*)-**10** (cyan carbons, in conformation *trans*-**III**).

fragment, the methoxy group and the phenyl ring was observed (Figure 5b). These superpositions imply that pharmacophore models for agonists and for MT_2-selective antagonists share the same arrangement of the common elements. This hypothesis obviously needs to be supported by further experimental data.

The enantiomer of **4b** that best fits the requirements of the chiral pharmacophore model for agonists is the (2*S*,4*S*) one (Figure 5a). This is consistent with the fact that the agonist 8-M-PDOT showed high stereoselectivity, with the (*S*)-enantiomer being the eutomer.[41] The *trans*-isomer **10** able to give a strict superposition of its 4-phenyl ring with that of the (2*S*,4*S*)-enantiomer of **4b** is the (2*R*,4*S*)-enantiomer, having opposite configuration of the amide chain (Figure 5c). The same orientation of the amide fragments of the two stereoisomers was achieved by selecting for **10** a H2−C2−N−H dihedral that, although consistent with NMR data, was unfavored at SD simulation. In particular, the conformation of **10** reported in Figure 5c has an equatorial arrangement of the amide chain and the NH bond pointing toward H2. This was a minimum-energy conformation, belonging to a family of similar snapshots, accounting for about 0.5% of the simulation ensemble (Table 4, *trans*-**III** in Figure 3). This unfavorable energetic state could explain, at least in part, the lower potency observed for the *trans* racemate **10**.

Model Validation: 4-P-PDOT Stereoisomers and Dihydronaphthalene Derivatives. The present availability of all four single 4-P-PDOT stereoisomers[30] allowed us to test them in the same experimental conditions employed for racemates **4b**, **4c**, and **10**. Their binding affinity and intrinsic

dx.doi.org/10.1021/jm200790v | *J. Med. Chem.* 2011, 54, 8362−8372

activity for MT_1 and MT_2 receptors are reported in Table 1. As predicted by the superpositions discussed above, the eutomers for the *cis* and *trans* racemic mixtures were the (2*S*,4*S*) and the (2*R*,4*S*) ones, respectively. The present data suggest that, also for MT_2-selective antagonists or partial agonists, the NH bond of the amide fragment should be arranged in an orientation perpendicular to the aromatic portion of the tetralin nucleus, pointing toward the same direction identified for MT_1/MT_2 agonists (Figure 5b). This hypothesis was further validated by testing compounds **3a** and **3b**, where the introduction of a double bond between positions 1 and 2 of the tetralin nucleus caused partial conjugation with the amide NH, preventing its perpendicular orientation. As expected, **3a** showed a significant loss of MT_2 receptor affinity (Table 2) compared to **4a**, **10**, and 4-P-PDOT racemates, in spite of the coplanar arrangement of the amide chain, that could resemble the equatorial one of 4-P-PDOT. Moreover, the introduction of the 8-methoxy group in **3b** did not improve MT_2 binding affinity, suggesting that these compounds interact with their binding site with poses differing from those required by the pharmacophore model discussed above. To further validate the hypothesis that this behavior is due to the nonperpendicular orientation of the amide fragment, a new compound was devised conserving the dihydronaphthalene nucleus but introducing a flexible methylene spacer, thus allowing close superposition of the aromatic and polar pharmacophore elements on those of *cis*-4-P-PDOT (Figure 6).

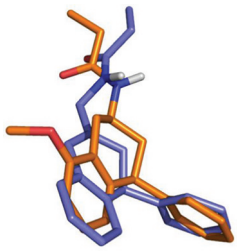

Figure 6. Superposition of *cis*-(2*S*,4*S*)-**4b** (orange carbons) and **6** (purple carbons).

Again, the predicted recovery of MT_2 binding affinity was observed for **6**, which behaved as a moderately selective MT_2 antagonist. Although the preferred way to confirm bioactive conformations is to prepare active compounds with constrained conformations, in this case we had indirect evidence on the role of NH orientation: compounds **3a** and **3b**, where rotation of the amide group is constrained in an orientation different from the putative active one, were inactive, while the flexible analogue **6**, topologically different from starting compounds and yet easily superimposable to the putative active conformation of **4b**, significantly recovered receptor affinity.

CONCLUSIONS

The present work reports some evidence supporting the hypothesis that melatonin receptor agonists and MT_2-selective antagonists or partial agonists share the same arrangement of their common pharmacophore elements. In particular, a 8-methoxy group on the scaffold of 4-P-PDOT conferred a significant increase of binding affinity, similar to what had been reported for the nonselective agonist 8-M-PDOT, conserved the *cis* > *trans* affinity rank, and could be bioisosterically replaced by a bromine atom. The effect of this group, suggesting the same binding role as in melatonin receptor agonists, prompted the superposition of accessible conformations of 8-methoxy-4-P-PDOT on the recently proposed active conformation of melatonin. The best matches of the common binding elements were observed for the most populated conformation of the (2*S*,4*S*)-*cis*-tetralin derivative and for an energetically unfavored conformation of the (2*R*,4*S*)-*trans* one. Binding studies on each single 4-P-PDOT stereoisomer and on appropriately designed, conformationally constrained dihydronaphthalene derivatives validated the proposed pharmacophore model.

EXPERIMENTAL SECTION

Chemistry. Melting points were determined on a Buchi B-540 capillary melting point apparatus and are uncorrected. ^{1}H NMR (200 or 600 MHz) and ^{13}C NMR (50 MHz) spectra were recorded on a Bruker AVANCE 200 or on a Varian INOVA 600 MHz spectrometer, using $CDCl_3$ as solvent unless stated otherwise. Chemical shifts (δ scale) are reported in parts per million (ppm) relative to the central peak of the solvent. Coupling constants (J) are given in hertz (Hz). EI-MS spectra (70 eV) were taken on a Fisons Trio 1000 instrument; only molecular ions (M^+) and base peaks are given. ESI-MS spectra were taken on a Waters Micromass Zq instrument; only molecular ions (M + 1) are given. Infrared spectra were obtained on a Nicolet Avatar 360 FT-IR spectrometer; absorbances are reported in cm^{-1}. Elemental analyses for C, H, and N were performed on a Carlo Erba analyzer. Purity of tested compounds was greater than 95%. Column chromatography purifications were performed under "flash" conditions using Merck 230−400 mesh silica gel. Analytical thin-layer chromatography (TLC) was carried out on Merck silica gel 60 F_{254} plates. The two radioligands 2-[^{125}I]iodomelatonin (specific activity, 2000 Ci/mmol) and [^{35}S]GTPγS ([^{35}S]guanosine 5′-*O*-(3-thiotriphosphate); specific activity, 1000 Ci/mmol) were purchased from Perkin-Elmer (Italy).

General Procedure for the Synthesis of Tetralones 2a−c. Freshly distilled styrene (0.69 mL, 6 mmol) in dry dichloromethane (70 mL) was added dropwise under nitrogen to an ice-cooled and stirred suspension of anhydrous aluminum chloride (1.6 g, 12 mmol) and the suitable phenylacetyl chloride (6 mmol) in dry dichloromethane (80 mL) (for the synthesis of tetralone **2b** we needed to change the adding order of the reagents: anhydrous aluminum trichloride was added to a cooled solution of styrene and 2-methoxyphenylacetyl chloride[42]). The mixture was stirred at 0 °C for a further 15 min, quenched by water, and extracted with CH_2Cl_2. The organic phases were combined, washed with brine, dried over Na_2SO_4, and concentrated under reduced pressure to afford the crude tetralone which was purified by flash chromatography (silica gel, cyclohexane−EtOAc, 9:1).

(±)-4-Phenyl-3,4-dihydronaphtalen-2(1*H*)-one (2a). Chemical physical data were identical with those previously reported.[31]

(±)-8-Methoxy-4-phenyl-3,4-dihydronaphtalen-2(1*H*)-one (2b). Oil; 35% yield. ESI MS (m/z): 253 (M + 1). ^{1}H NMR (200 MHz, $CDCl_3$): δ 2.94 (d, 2H, J = 6.2), 3.53 (d, 1H, J = 21.8), 3.65 (d, 1H, J = 21.8), 3.87 (s, 3H), 4.47 (dd, 1H, J = 6.0), 6.66 (d,1H, J = 7.7), 6.81 (d, 1H, J = 8.1), 7.08−7.35 (m, 6H). ^{13}C NMR (50 MHz, $CDCl_3$): δ 38.2, 45.4, 46.5, 55.4, 108.4, 120.6, 122.2, 126.9, 127.4, 127.8, 128.8, 139.9, 142.2, 156.8, 209.5.

(±)-8-Bromo-4-phenyl-3,4-dihydronaphtalen-2(1*H*)-one (2c). Oil; 34% yield. MS (EI): m/z 300−302 (M^+), 178 (100). ^{1}H NMR (200 MHz, $CDCl_3$): δ 2.92 (dd, 1H, J = 6.2 and J = 15.7), 3.01 (dd, 1H, J = 6.2 and = 15.7), 3.66 (d, 1H, J = 21.4), 3.79 (d, 1H, J = 21.4), 4.50 (dd, 1H, J = 6.2), 6.81−7.12 (m, 5H), 7.30−7.34 (m, 2H), 7.54 (dd, 1H, J = 1.4 and J = 7.6). ^{13}C NMR (50 MHz, $CDCl_3$): δ 44.7, 45.6, 46.1, 124.6, 127.2, 127.7, 128.1, 128.2, 129.0, 131.3, 133.2, 141.2, 141.4, 207.7.

General Procedure for the Synthesis of Enamides 3a−c. A solution of the suitable tetralone **2a−c** (6.8 mmol), propionamide (1.2 g, 16.4 mmol), and *p*-toluenesulfonic acid (0.13 g, 0.7 mmol) in toluene (30 mL) was refluxed for 4 h under nitrogen atmosphere in a 50 mL round-bottom flask equipped with a Dean−Stark apparatus. After the mixture was cooled to room temperature, the propionamide

was precipitated and filtered off. The organic phase was washed with a saturated solution of $NaHCO_3$ (3 × 50 mL) and water (3 × 50 mL), dried over Na_2SO_4, and concentrated under reduced pressure to give a crude residue that was purified by flash chromatography (silica gel, cyclohexane−EtOAc, 7:3) and crystallization.

(±)-*N*-(4-Phenyl-3,4-dihydronaphtalen-2-yl)propionamide (3a). Chemical physical data were identical with those previously reported.[31]

(±)-*N*-(8-Methoxy-4-phenyl-3,4-dihydronaphtalen-2-yl)-propionamide (3b). White solid, mp 195−196 °C (acetone/Et_2O); 52% yield. ESI MS (*m*/*z*): 308 (M + 1). ^{1}H NMR (200 MHz, $CDCl_3$): δ 1.18 (t, 3H, *J* = 7.4), 2.29 (q, 2H, *J* = 7.4), 2.74 (dd, 1H, *J* = 8.6 and *J* = 16.4), 2.84 (dd, 1H, *J* = 7.2 and *J* = 16.4), 3.86 (s, 3H), 4.19 (dd, 1H, *J* = 8.6 and *J* = 7.2), 6.44 (d, 1H, *J* = 7.6), 6.54 (br s, 1H), 6.74 (d, 1H, *J* = 8.2), 7.00 (dd, 1H, *J* = 7.2 and *J* = 8.5), 7.20−7.35 (m, 6H). ^{13}C NMR (50 MHz, $CDCl_3$): δ 9.5, 30.8, 35.3, 44.4, 55.5, 109.0, 120.0, 123.6, 126.4, 126.6, 128.3, 128.5, 130.0, 133.0, 136.5, 143.6, 154.7, 172.1. IR (cm^{-1}, Nujol): 3344, 1662. Anal. ($C_{20}H_{21}NO_2$) C, H, N.

(±)-*N*-(8-Bromo-4-phenyl-3,4-dihydronaphtalen-2-yl)-propionamide (3c). White solid, mp 133−134 °C (acetone/petroleum ether); 55% yield. MS (EI): *m*/*z* 355−357 (M^+), 57 (100). ^{1}H NMR (200 MHz, acetone-d_6): δ 1.18 (t, 3H, *J* = 7.5), 2.31 (q, 2H, *J* = 7.5), 2.76 (dd, 1H, *J* = 8.3 and *J* = 16.4), 2.87 (dd, 1H, *J* = 8.3 and *J* = 16.4), 4.19 (dd, 1H, *J* = 8.3), 6.46 (br s, 1H), 6.75−6.90 (m, 3H), 7.16−7.47 (m, 6H). ^{13}C NMR (50 MHz, $CDCl_3$): δ 9.3, 30.6, 35.1, 44.8, 109.7, 121.9, 126.6, 126.7, 126.9, 128.2, 128.6, 131.2, 134.1, 135.9, 137.7, 142.8, 172.3.

General Procedure for the Synthesis of Tetralines 4a−c. Triethylsilane (0.4 mL, 2.5 mmol) was added dropwise to a cooled (−10 °C) solution of the suitable enamide **3a−c** (0.25 mmol) in CF_3COOH (3.25 mL), and the resulting mixture was stirred for a further 10 min at −10 °C. A saturated aqueous solution of $NaHCO_3$ was carefully added until neutral pH, and the resulting mixture was extracted with CH_2Cl_2 (3 × 50 mL). The combined organic extracts were washed with brine (3 × 50 mL), dried over Na_2SO_4, and concentrated under reduced pressure to give a crude residue that was purified by flash cromatography (silica gel, cyclohexane−ethyl acetate, 7:3).

(±)-*cis*-*N*-(4-Phenyl-1,2,3,4-tetrahydronaphtalen-2-yl)-propionamide (4a, 4-P-PDOT). Chemical physical data were identical with those previously reported.[31]

(±)-*cis*-*N*-(8-Methoxy-4-phenyl-1,2,3,4-tetrahydronaphtalen-2-yl)propionamide (4b). Mixture of *cis* and *trans* diastereomers (*cis*/*trans* ratio 80/20 by HPLC analysis) was obtained from which the pure (±)-*cis*-**4b** can be obtained by a single recrystallization (acetone/*n*-hexane). White solid, mp 220−222 °C; 60% yield. ESI MS (*m*/*z*): 310 (M + 1). ^{1}H NMR (600 MHz, $CDCl_3$): δ 1.10 (t, 3H, *J* = 7.2, $CH_2\underline{CH_3}$), 1.71 (ddd, 1H, *J* = 12.0, H3b), 2.31 (m, 2H, $\underline{CH_2}CH_3$), 2.34 (ddd, 1H, *J* = 2.4, 4.8, and 12.0, H3a), 2.38 (dd, 1H, *J* = 10.8 and 16.8, H1b), 3.29 (dd, 1H, *J* = 5.4 and 16.8, H1a), 3.79 (s, 3H, OCH_3), 4.19 (dd, 1H, *J* = 4.8 and 12.0, H4), 4.29 (m, 1H, H2), 5.38 (br d, 1H, *J* = 7.2, NH), 6.50 (d, 1H *J* = 7.8, H5), 6.64 (d, 1H, *J* = 8.7, H7), 6.97 (dd, 1H, *J* = 7.8 and 8.4, H6), 7.10 (d, 2H, *J* = 7.8, Ho), 7.18 (dd, 1H, *J* = 7.2, Hp), 7.25 (dd, 2H, *J* = 7.2, Hm). ^{13}C NMR (50 MHz, $CDCl_3$): δ 9.9, 29.9, 30.7, 39.9, 45.5, 46.2, 55.3, 107.2, 121.6, 124.1, 126.4, 128.4, 128.5, 128.6, 140.1, 146.0, 156.9, 173.1. IR (cm^{-1}, Nujol): 3336, 1646. Anal. ($C_{20}H_{23}NO_2$) C, H, N.

(±)-*cis*-*N*-(8-Bromo-4-phenyl-1,2,3,4-tetrahydronaphtalen-2-yl)propionamide (4c). Mixture of *cis* and *trans* diastereomers (*cis*/*trans* ratio 90/10 by HPLC analysis) was obtained from which the pure (±)-*cis*-**4c** can be obtained by a single recrystallization (acetone/*n*-hexane). White solid, mp 196−197 °C; 54% yield. ESI MS (*m*/*z*): 358−360 (M + 1). ^{1}H NMR (200 MHz, $CDCl_3$): δ 1.16 (t, 3H, *J* = 7.6), 1.76 (ddd, 1H, *J* = 12.0), 2.21 (q, 2H, *J* = 7.6), 2.35 (ddd, 1H, *J* = 3.0, *J* = 5.0, and *J* = 12.0), 2.59 (dd, 1H, *J* = 11.3 and *J* = 16.0), 3.39 (dd, 1H, *J* = 5.0 and *J* = 16), 4.25 (dd, 1H, *J* = 5.0 and *J* = 12), 4.41 (dddd, 1H, *J* = 3.0, 5.0, 8.5 and *J* = 12), 5.49 (br d, 1H, *J* = 8.4), 6.75 (d, 1H, *J* = 8.0), 6.92 (dd, 1H, *J* = 8.0), 7.10−7.15 (m, 2H), 7.21−7.44 (m, 4H). ^{13}C NMR (50 MHz, $CDCl_3$): δ 9.8, 29.8, 37.6, 39.8, 45.6, 46.6, 125.3, 126.6, 127.3, 128.6, 128.7, 128.8, 130.4, 134.6, 141.6, 145.4, 173.1. IR (cm^{-1}, Nujol): 3302, 1639. Anal. ($C_{19}H_{20}BrNO$) C, H, N.

4-Phenyl-3,4-dihydronaphtalene-2-carbonitrile (5). A solution of **2a** (0.75 g, 3.38 mmol), trimethylsilyl cyanide (0.58 mL, 4.35 mmol), and ZnI_2 (0.027 g, 0.081 mmol) in toluene (2.5 mL) was stirred at room temperature for 18 h. Pyridine (5 mL) and afterward $POCl_3$ (1 mL, 11 mmol) were added to the above solution, and the resulting mixture was refluxed for 1 h. After cooling, the reaction mixture was poured into 5% HCl/ice and the aqueous phase was extracted with EtOAc. The combined organic extracts were washed with brine, dried (Na_2SO_4), and concentrated under reduced pressure to give a crude residue that was purified by flash chromatography (silica gel, cyclohexane/EtOAc, 9:1 as eluent). Oil, 38% yield. ESI MS (*m*/*z*): 232 (M + 1). ^{1}H NMR (200 MHz, $CDCl_3$): δ 2.81 (ddd, 1H, *J* = 1.5, 9.5 and *J* = 16.8), 2.90 (ddd, 1H, *J* = 1.5, 7.5 and *J* = 16.8), 4.25 (dd, 1H, *J* = 7.5 and *J* = 9.5), 6.80−7.65 (m, 10H).

***N*-[(4-Phenyl-3,4-dihydronaphthalen-2-yl)methyl]propionamide (6).** A 1 M solution of $LiAlH_4$ in diethyl ether (1.3 mL, 1.3 mmol) was added dropwise to a solution of **5** (0.3 g, 1.3 mmol) in dry diethyl ether (4 mL). The reaction mixture was stirred at room temperature for 15 min and then quenched by water and a 15% NaOH aqueous solution. The mixture was extracted with EtOAc, and the combined organic phases were washed with brine, dried (Na_2SO_4), and concentrated under reduced pressure. The obtained crude residue was dissolved in THF (14 mL), and to the mixture were added TEA (0.23 mL, 1.64 mmol) and propionic anhydride (0.21 mL, 1.64 mmol). The resulting solution was stirred at room temperature for 16 h. After distillation of the solvent under reduced pressure, the residue was partitioned between EtOAc and 2 N NaOH. The organic layer was washed with brine, dried (Na_2SO_4), and concentrated under reduced pressure to give a crude residue which was purified by flash chromatography (silica gel, CH_2Cl_2−acetone, 95:5) and crystallization. White solid, mp 118−120 °C (EtOAc−petroleum ether); 46% yield. MS (EI): *m*/*z* 291 (M^+), 218 (100). ^{1}H NMR (200 MHz, $CDCl_3$): δ 1.10 (t, 3H, *J* = 7.6), 2.14 (q, 2H, *J* = 7.6), 2.51 (dd, 1H, *J* = 8.0 and *J* = 16.5), 2.67 (dd, 1H, *J* = 7.0 and *J* = 16.5), 3.90 (dd, 1H, *J* = 4.5, and *J* = 15.0), 4.03 (dd, 1H, *J* = 6.5, and *J* = 15.0), 4.16 (dd, 1H, *J* = 7.0, and *J* = 8.0), 5.25 (br t, 1H), 6.41 (s, 1H), 6.89 (d, 1H, *J* = 6.8), 7.12−7.33 (m, 8H). ^{13}C NMR (50 MHz, $CDCl_3$): δ 9.8, 29.7, 34.0, 43.9, 44.3, 124.1, 126.2, 126.5, 127.0, 127.4, 127.9, 128.2, 128.4, 134.0, 135.6, 137.0, 144.0, 173.7. IR (cm^{-1}, Nujol): 3307, 1643. Anal. ($C_{20}H_{21}NO$) C, H, N.

(±)-*cis*-8-Methoxy-4-phenyl-1,2,3,4-tetrahydronaphtalen-2-ol (7). $NaBH_4$ (0.105 g, 2.8 mmol) was added portionwise to an ice-cooled stirred solution of **2b** (0.2 g, 0.8 mmol) in dry MeOH (6 mL), and the resulting mixture was heated at reflux for 16 h. After the mixture was cooled to room temperature, water was added and MeOH was removed by distillation under reduced pressure. The residue was extracted with CH_2Cl_2 (3 × 50 mL). The combined organic phases were washed with brine, dried (Na_2SO_4), and concentrated to afford the crude alcohols (*cis*/*trans*, 85/15, by ^{1}H NMR analysis) which were purified by flash chromatography (silica gel, cyclohexane−EtOAc, 7:3). Oil, 59% yield. ESI MS (*m*/*z*): 255 (M + 1). ^{1}H NMR (±)-*cis*-isomer (200 MHz, $CDCl_3$): δ 1.64 (brs, 1H), 1.91 (ddd, 1H, *J* = 12.0), 2.37 (ddd, 1H, *J* = 3.0, 5.5 and *J* = 12.0), 2.55 (dd, 1H, *J* = 10.0 and *J* = 16.5), 3.37 (dd, 1H, *J* = 5.5 and *J* = 16.5), 3.86 (s, 3H), 4.10−4.21 (m, 2H), 6.37 (d, 1H, *J* = 7.8), 6.69 (d, 1H, *J* = 7.8), 7.01 (t, 1H, *J* = 7.8), 7.15−7.38 (m, 5H). ^{13}C NMR (50 MHz, $CDCl_3$): δ 33.4, 42.6, 46.5, 55.4, 67.9, 107.3, 121.3, 126.3, 126.4, 128.5, 128.7, 140.2, 146.0, 157.0, 157.9.

(±)-*cis*-8-Methoxy-4-phenyl-1,2,3,4-tetrahydronaphtalen-2-yl-4-methylbenzensulfonate (8). A solution of *p*-toluensulfonyl chloride (0.15 g, 0.78 mmol) in dry pyridine (1.15 mL) was added to a solution of (±)-*cis*-7 (0.100 g, 0.39 mmol) in dry pyridine (1.15 mL), and the resulting mixture was stirred at 5 °C for 3 days. The mixture was poured into ice−water. The resulting precipitate was filtered, washed with water, and dried to afford the desired *cis*-tosylate which was used for the next step without any further purification. Amorphous solid; 82% yield. ESI MS (*m*/*z*): 426 (M + NH_4). ^{1}H NMR (±)-*cis*-isomer (200 MHz, $CDCl_3$): δ 2.09 (ddd, 1H, *J* = 12.0), 2.31−2.40 (m,

dx.doi.org/10.1021/jm200790v | *J. Med. Chem.* 2011, 54, 8362−8372

1H), 2.46 (s, 3H), 2.79 (dd, 1H, J = 10.5, J = 16.5), 3.28 (dd, 1H, J = 16.5 and J = 6.0), 3.81 (s, 3H), 4.09 (dd, 1H, J = 5.5 and J = 12.0), 4.85 (dddd, 1H, J = 6.0, 10.5 and J = 12.0), 6.32 (d, 1H, J = 7.9), 6.66 (d, 1H, J = 7.9), 7.00 (t, 1H, J = 7.9), 7.09−7.31 (m, 5H), 7.35 (d, 2H, J = 8.3), 7.83 (d, 2H, J = 8.3).

(±)-*trans*-*N*-(8-Methoxy-4-phenyl-1,2,3,4-tetrahydronaphtalen-2-yl)propionamide (10). A solution of sodium azide (0.106 g, 1.7 mmol) in water (1 mL) was added dropwise to a stirred solution of **8** (0.13 g, 0.32 mmol) in DMF (1.1 mL), and the resulting mixture was stirred for 5 h at 45−50 °C. The reaction mixture was poured into ice−water and extracted with CH_2Cl_2 (3 × 50 mL). The combined organic extracts were washed with brine, dried (Na_2SO_4), and concentrated to afford the crude azido intermediate **9** which was sufficiently pure to be used without any further purification. EI MS (m/z): 279 (M^+), 236 (M^+, 100). ^{1}H NMR (±)-*trans*-isomer (200 MHz, $CDCl_3$): δ 2.17 (dd, 1H, J = 6.0 and J = 14.0), 2.38−2.47 (m, 1H), 2.73−2.86 (m, 1H), 3.18 (dd, 1H, J = 5.0 and J = 18.0), 3.88 (s, 3H), 3.88−4.04 (m, 1H), 4.35 (t, 1H, J = 6.0), 6.54 (d, 1H, J = 7.8), 6.74 (d, 1H, J = 7.8), 6.97−7.31 (m, 6H).

A solution of the above crude azide **9** in *i*-PrOH (7.8 mL) and CH_2Cl_2 (0.4 mL) was hydrogenated in the presence of 10% Pd/C at 4 atm of H_2 for 16 h at room temperature. The catalyst was removed by filtration on Celite. The filtrate was concentrated to afford a crude oily amine, which was used without any further purification. TEA (0.06 mL, 0.43 mmol) and propionic anhydride (0.05 mL, 0.4 mmol) were added to a cold solution of the above crude amine in THF (4.5 mL), and the resulting mixture was stirred at room temperature for 4 h. The solvent was removed by distillation under reduced pressure, and the resulting crude amide was purified by flash chromatography (silica gel, CH_2Cl_2−acetone, 95:5). Amorphous solid; 25% overall yield. ESI MS (m/z): 310 (M + 1). ^{1}H NMR (600 MHz, $CDCl_3$): δ 1.09 (t, 3H, J = 7.8, $CH_2\underline{CH_3}$), 1.99 (ddd, 1H, J = 3.0, 7.2 and 12.6, H3a), 2.12 (q, 2H, J = 7.6, $\underline{CH_2}CH_3$), 2.17 (ddd, 1H, J = 6.0, 7.8 and 12.6, H3b), 2.56 (dd, 1H, J = 6.0 and J = 17.4, H1b), 3.16 (dd, 1H, J = 5.4 and J = 17.4, H1a), 3.80 (s, 3H, OCH_3), 4.17 (dd, 1H, J = 6.6, H4), 4.32 (m, 1H, H2), 5.40 (br d, 1H, J = 7.2, NH), 6.50 (d, 1H, J = 7.8, H5), 6.67 (d, 1H, J = 7.8, H7), 7.02 (d, 2H, J = 7.2, Ho), 7.04 (t, 1H, J = 7.8, H6), 7.15 (dd, 1H, J = 7.2, Hp), 7.22 (dd, 2H, J = 7.8, Hm). ^{13}C NMR (50 MHz, $CDCl_3$): δ 9.8, 29.80, 29.83, 36.9, 42.2, 43.0, 55.3, 107.3, 122.2, 123.7, 126.5, 126.6, 128.4, 128.7, 139.0, 146.0, 157.4, 173.2. Anal. ($C_{20}H_{23}NO_2$) C, H, N.

Pharmacology. Binding affinities were determined using 2-[^{125}I]iodomelatonin as the labeled ligand in competition experiments on cloned human MT_1 and MT_2 receptors expressed in NIH3T3 rat fibroblast cells. The characterization of NIH3T3-MT_1 and -MT_2 cells had been already described in detail.[21,43] Membranes were incubated for 90 min at 37 °C in binding buffer (Tris-HCl, 50 mM, pH 7.4). The final membrane concentration was 5−10 μg of protein per tube. The membrane protein level was determined in accordance with a previously reported method.[44] 2-[^{125}I]Iodomelatonin (100 pM) and different concentrations of melatonin (10^{-10}−10^{-6} M) or of the new compounds were incubated with the receptor preparation for 90 min at 37 °C. Nonspecific binding was assessed with 10 μM melatonin; IC_{50} values were determined by nonlinear fitting strategies with the program PRISM (GraphPad SoftWare Inc., San Diego, CA). The pK_i values were calculated from the IC_{50} values in accordance with the Cheng−Prusoff equation.[45] The pK_i values are the mean of at least three independent determinations performed in duplicate.

To define the functional activity of the new compounds at MT_1 and MT_2 receptor subtypes, [^{35}S]GTPγS binding assays in NIH3T3 cells expressing human-cloned MT_1 or MT_2 receptors were performed. The amount of bound [^{35}S]GTPγS is proportional to the level of the analogue-induced G-protein activation and is related to the intrinsic activity of the compound under study. The detailed description and validation of this method were reported elsewhere.[43,46] Membranes (15−25 μg of protein, final incubation volume 100 μL) were incubated at 30 °C for 30 min in the presence and in the absence of melatonin analogues in an assay buffer consisting of [^{35}S]GTPγS (0.3−0.5 nM), GDP (50 μM), NaCl (100 mM), and $MgCl_2$ (3 mM). Nonspecific binding was defined using [^{35}S]GTPγS (10 μM). In cell lines expressing human MT_1 or MT_2 receptors, melatonin produced a concentration dependent stimulation of basal [^{35}S]GTPγS binding with a maximal stimulation, above basal levels, of 370% and 250% in MT_1 and MT_2 receptors, respectively. Basal stimulation is the amount of [^{35}S]GTPγS specifically bound in the absence of compounds, and it was taken as 100%. The maximal G-protein activation was measured in each experiment by using melatonin (100 nM). Compounds were added at three different concentrations (one concentration was equivalent to 100 nM melatonin, a second one 10 times smaller, and a third one 10 times larger), and the percent stimulation above basal was determined. The equivalent concentration was estimated on the basis of the ratio of the affinity of the test compound to that of melatonin. It was assumed that at the equivalent concentration the test compound occupies the same number of receptors as 100 nM melatonin. All of the measurements were performed in triplicate. The relative intrinsic activity (IAr) values were obtained by dividing the maximum ligand-induced stimulation of [^{35}S]GTPγS binding by that of melatonin as measured in the same experiment. By convention, the natural ligand melatonin has an efficacy (E_{max}) of 100%. Full agonists stimulate [^{35}S]GTPγS binding with a maximum efficacy, close to that of melatonin itself. If E_{max} is between 30% and 70% that of melatonin (0.3 < IAr < 0.7), the compound is considered a partial agonist, whereas if E_{max} is lower than 30% (IAr < 0.3), the compound is considered an antagonist.[37]

NMR Spectroscopy. NMR spectra of compounds **4b** and **10** were recorded on a Varian INOVA 600 MHz spectrometer. The sample concentration used in NMR studies was about 5 mM dissolved in deuterated chloroform. 1D and 2D NMR spectra were measured at 298 K. ^{1}H chemical shifts were given on the δ scale and were calibrated to the residual solvent signal of $CDCl_3$ at δ 7.22. NOESY spectra are reported in Supporting Information (Figures S1 and S2).

Molecular Modeling. Molecular modeling studies were performed with Macromodel 9.7.[47] Starting structures of **4b** and **10** stereoisomers were optimized with the MM2 force field,[48] using a convergence criterion of 0.2 kJ mol^{-1} Å^{-1}, applying the GB/SA[49] $CHCl_3$ solvation treatment. Stochastic dynamics (SD) simulations were performed employing the MM2 force field with implicit $CHCl_3$, applying a time step of 1 fs and a temperature of 298 K for 1 μs after 1000 ps of equilibration; 50 000 snapshots were collected for data analysis. SD had already proved to be able to reproduce the conformational equilibrium of small molecules in $CHCl_3$, applying an implicit treatment of solvent molecules.[50−56] Preliminary SD simulations performed on both enantiomers of **4b** and **10** gave comparable results for each couple of enantiomers in terms of relative abundances of different conformations. Therefore, full-length SD simulations were conducted on two reference enantiomers only, i.e., (2*S*,4*S*)-**4b** and (2*R*,4*S*)-**10**. For the *trans* derivative (2*R*,4*S*)-**10**, different starting conformations were tested, with axial amide side chain and pseudoequatorial phenyl substituent or with equatorial amide side chain and pseudoaxial phenyl substituent. The starting point did not significantly affect the results.

Proton−proton coupling constants of **4b** and **10** were calculated with the software Maestro 9.0,[57] applying the implemented version of the Karplus equation[58] to the dihedrals of single conformations collected during SD simulations. The expected values of coupling constants reported in Table 3 are average values for 50 000 conformations, unless otherwise indicated.

Superposition of compounds was performed by means of a rigid fit procedure, superimposing the four atoms of the amide function, the centroid of the phenyl rings, and the oxygen atom of the methoxy group, when present.

■ ASSOCIATED CONTENT

Ⓢ Supporting Information

NOESY spectra for compounds **4b** and **10**, results of stochastic dynamics simulations on **4b** and **10**, and elemental analytical data. This material is available free of charge via the Internet at http://pubs.acs.org.

AUTHOR INFORMATION

Corresponding Author

*Phone: +39 0521 905062. Fax: +39 0521 905006. E-mail: silvia.rivara@unipr.it.

ACKNOWLEDGMENTS

We are grateful to the Centro Interdipartimentale Misure "Giuseppe Casnati" of the University of Parma, Italy, for providing NMR instrumentation.

ABBREVIATIONS USED

8-M-PDOT, 8-methoxy-2-propionamidotetralin; 4-P-PDOT, 4-phenyl-2-propionamidotetralin; cAMP, cyclic adenosine monophosphate; DMF, dimethylformamide; GTPγS, guanosine 5′-*O*-(3-thiotriphosphate); IAr, relative intrinsic activity; MT_1, melatonin receptor subtype 1; MT_2, melatonin receptor subtype 2; NOE, nuclear Overhauser effect; NOESY, nuclear Overhauser effect spectroscopy; PTSA, *p*-toluenesulfonic acid; SAR, structure−activity relationship; SD, stochastic dynamics; TEA, triethylamine; THF, tetrahydrofuran; TFA, trifluoroacetic acid

REFERENCES

(1) Arendt, J. Melatonin: Characteristics, Concerns, and Prospects. *J. Biol. Rhythms* **2005**, *20*, 291−303.

(2) Scheer, F. A.; Van Montfrans, G. A.; Van Someren, E. J.; Mairuhu, G.; Buijs, R. M. Daily Nighttime Melatonin Reduces Blood Pressure in Male Patients with Essential Hypertension. *Hypertension* **2004**, *43*, 192−197.

(3) Carrillo-Vico, A.; Reiter, R. J.; Lardone, P. J.; Herrera, J. L.; Fernandez-Montesinos, R.; Guerrero, J. M.; Pozo, D. The Modulatory Role of Melatonin on Immune Responsiveness. *Curr. Opin. Invest. Drugs* **2006**, *7*, 423−431.

(4) Satomura, K; Tobiume, S.; Tokuyama, R.; Yamasaki, Y.; Kudoh, K.; Maeda, E.; Nagayama, M. Melatonin at Pharmacological Doses Enhances Human Osteoblastic Differentiation in Vitro and Promotes Mouse Cortical Bone Formation in Vivo. *J. Pineal Res.* **2007**, *42*, 231−239.

(5) Barrenetxe, J.; Delagrange, P.; Martinez, J. A. Physiological and Metabolic Functions of Melatonin. *J. Physiol. Biochem.* **2004**, *60*, 61−72.

(6) Turek, F. W.; Gillette, M. U. Melatonin, Sleep, and Circadian Rhythms: Rationale for Development of Specific Melatonin Agonists. *Sleep Med.* **2004**, *5*, 523−532.

(7) Mills, E.; Wu, P.; Seely, D.; Guyatt, G. Melatonin in the Treatment of Cancer: A Systematic Review of Randomized Controlled Trials and Meta-Analysis. *J. Pineal Res.* **2005**, *39*, 360−366.

(8) Medeiros, C. A. M.; Carvalhedo de Bruin, P. F.; Lopes, L. A.; Magalhães, M. C.; Seabra, M.; de, L.; Sales de Bruin, V. M. Effect of Exogenous Melatonin on Sleep and Motor Dysfunction in Parkinson's Disease. A Randomized, Double Blind, Placebo-Controlled Study. *J. Neurol.* **2007**, *254*, 459−464.

(9) Macleod, M. R.; O'Collins, T.; Horky, L. L.; Howells, D. W.; Donnan, G. A. Systematic Review and Meta-Analysis of the Efficacy of Melatonin in Experimental Stroke. *J. Pineal Res.* **2005**, *38*, 35−41.

(10) Reppert, S. M.; Weaver, D. R.; Godson, C. Melatonin Receptors Step into the Light: Cloning and Classification of Subtypes. *Trends Pharmacol. Sci.* **1996**, *17*, 100−102.

(11) Dubocovich, M. L.; Delagrange, P.; Krause, D. N.; Sugden, D.; Cardinali, D. P.; Olcese, J. International Union of Basic and Clinical Pharmacology. LXXV. Nomenclature, Classification, and Pharmacology of G Protein-Coupled Melatonin Receptors. *Pharmacol. Rev.* **2010**, *62*, 343−380.

(12) Nosjean, O.; Ferro, M.; Cogé, F.; Beauverger, P.; Henlin, J.-M.; Lefoulon, F.; Fauchère, J.-L.; Delagrange, P.; Canet, E.; Boutin, J. A. Enzyme Catalysis and Regulation. *J. Biol. Chem.* **2000**, *275*, 31311−31317.

(13) (a) Wade, A. G.; Ford, I.; Crawford, G.; McMahon, A. D.; Nir, T.; Laudon, M.; Zisapel, N. Efficacy of Prolonged Release Melatonin in Insomnia Patients Aged 55−80 Years: Quality of Sleep and Next-Day Alertness Outcome. *Curr. Med. Res. Opin.* **2007**, *23*, 2597−2605. (b) Neurim Pharamceuticals. http://www.neurim.com.

(14) Simpson, D.; Curran, M. P. Ramelteon, a Review of Its Use in Insomnia. *Drugs* **2008**, *68*, 1901−1919.

(15) (a) Yous, S.; Andrieux, J.; Howell, H. E.; Morgan, P. J.; Renard, P.; Pfeiffer, B.; Lesieur, D.; Guardiola-Lemaître, B. Novel Naphthalenic Ligands with High Affinity for the Melatonin Receptor. *J. Med. Chem.* **1992**, *35*, 1484−1486. (b) Kennedy, S.; Emsley, R. Placebo-Controlled Trial of Agomelatine in the Treatment of Major Depressive Disorder. *Eur. Neuropsychopharmacol.* **2006**, *16*, 93−100.

(16) Spadoni, G.; Bedini, A.; Mor, M.; Rivara, S. The Rationale for the Development of Melatonin Receptor Ligands. In *Sleep Disorders: Diagnosis and Therapeutics*; Pandi-Pemural, S. R., Verster, J. C., Monti, J. M., Lader, M. H., Langer, S. Z., Eds.; Informa Healthcare: London, 2008; pp 402−416.

(17) (a) Zlotos, D. P. Recent Advances in Melatonin Receptor Ligands. *Arch. Pharm. (Weinheim, Ger.)* **2005**, *338*, 229−247. (b) Garratt, P. J.; Tsotinis, A. Synthesis of Compounds As Melatonin Agonists and Antagonists. *Mini-Rev. Med. Chem.* **2007**, *7*, 1075−1088.

(18) Rivara, S.; Mor, M.; Bedini, A.; Spadoni, G.; Tarzia, G. Melatonin Receptor Agonists: SAR and Applications to the Treatment of Sleep−Wake Disorders. *Curr. Top. Med. Chem.* **2008**, *8*, 954−968.

(19) Koike, T.; Hoashi, Y.; Takai, T.; Nakayama, M.; Yukuhiro, N.; Ishikawa, T.; Hirai, K.; Uchikawa, O. 1,6-Dihydro-2*H*-indeno[5,4-*b*]furan Derivatives: Design, Synthesis, and Pharmacological Characterization of a Novel Class of Highly Potent MT_2-Selective Agonists. *J. Med. Chem.* **2011**, *54*, 3436−3444.

(20) Dubocovich, M. L.; Masana, M. I.; Iacob, S.; Sauri, D. M. Melatonin Receptor Antagonists That Differentiate between the Human Mel1a and Mel1b Recombinant Subtypes Are Used To Assess the Pharmacological Profile of the Rabbit Retina ML1 Presynaptic Heteroreceptor. *Naunyn Schmiedeberg's Arch. Pharmacol.* **1997**, *355*, 365−375.

(21) Nonno, R.; Pannacci, M.; Lucini, V.; Angeloni, D.; Fraschini, F.; Stankov, B. M. Ligand Efficacy and Potency at Recombinant Human MT_2 Melatonin Receptors: Evidence for Agonist Activity of Some MT_1-Antagonists. *Br. J. Pharmacol.* **1999**, *127*, 1288−1294.

(22) Browning, C.; Beresford, I.; Frasner, N.; Giles, H. Pharmacological Characterization of Human Recombinant Melatonin MT_1 and MT_2 Receptors. *Br. J. Pharmacol.* **2000**, *129*, 877−886.

(23) Audinot, V.; Mailliet, F.; Lahaye-Brasseur, C.; Bonnaud, A.; Le Gall, A.; Amossé, C.; Dromaint, S.; Rodriguez, M.; Nagel, N.; Galizzi, J. P.; Malpaux, B.; Guillaumet, G.; Lesieur, D.; Lefoulon, F.; Renard, P.; Delagrange, P.; Boutin, J. A. New Selective Ligands of Human Cloned Melatonin MT_1 and MT_2 Receptors. *Naunyn Schmiedeberg's Arch. Pharmacol.* **2003**, *367*, 553−561.

(24) Gatti, G.; Piersanti, G.; Spadoni, G. Conformation by NMR of Two Tetralin-Based Receptor Ligands. *Farmaco* **2003**, *58*, 469−476.

(25) Spadoni, G.; Balsamini, C.; Diamantini, G.; Tontini, A.; Tarzia, G.; Mor, M.; Rivara, S.; Plazzi, P. V.; Nonno, R.; Lucini, V.; Pannacci, M.; Fraschini, F.; Stankov, B. M. 2-*N*-Acylaminoalkylindoles: Design and Quantitative Structure−Activity Relationship Studies Leading to MT_2-Selective Melatonin Antagonists. *J. Med. Chem.* **2001**, *44*, 2900−2912.

(26) Rivara, S.; Diamantini, G.; Di Giacomo, B.; Lamba, D.; Gatti, G.; Lucini, V.; Pannacci, M.; Mor, M.; Spadoni, G.; Tarzia, G. Reassessing the Melatonin Pharmacophore—Enantiomeric Resolution, Pharmacological Activity, Structure Analysis, and Molecular Modeling of a Constrained Chiral Melatonin Analogue. *Bioorg. Med. Chem.* **2006**, *14*, 3383−3391.

(27) Mor, M.; Spadoni, G.; Di Giacomo, B.; Diamantini, G.; Bedini, A.; Tarzia, G.; Plazzi, P. V.; Rivara, S.; Nonno, R.; Lucini, V.; Pannacci, M.; Fraschini, F.; Stankov, B. M. Synthesis, Pharmacological

Characterization and QSAR Studies on 2-Substituted Indole Melatonin Receptor Ligands. *Bioorg. Med. Chem.* **2001**, *9*, 1045−1057.
(28) Lucini, V.; Pannacci, M.; Scaglione, F.; Fraschini, F.; Rivara, S.; Mor, M.; Bordi, F.; Plazzi, P. V.; Spadoni, G.; Bedini, A.; Piersanti, G.; Diamantini, G.; Tarzia, G. Tricyclic Alkylamides as Melatonin Receptor Ligands with Antagonist or Inverse Agonist Activity. *J. Med. Chem.* **2004**, *47*, 4202−4212.
(29) Rivara, S.; Lodola, A.; Mor, M.; Bedini, A.; Spadoni, G.; Lucini, V.; Pannacci, M.; Fraschini, F.; Scaglione, F.; Ochoa Sanchez, R.; Gobbi, G.; Tarzia, G. N-(Substituted-anilinoethyl)amides: Design, Synthesis, and Pharmacological Characterization of a New Class of Melatonin Receptor Ligands. *J. Med. Chem.* **2007**, *50*, 6618−6626.
(30) Lucarini, S.; Bartolucci, S.; Bedini, A.; Gatti, G.; Orlando, P.; Piersanti, G.; Spadoni G. Synthesis and Configuration Determination of All Enantiopure Stereoisomers of the Melatonin Receptor Ligand 4-Phenyl-2-propionamidotetralin Using an Expedient Optical Resolution of 4-Phenyl-2-tetralone. *Org. Biomol. Chem.* [Online early access]. DOI: 10.1039/C1OB06369C. Published Online: Sep 30, **2011**.
(31) Lucarini, S.; Bedini, A.; Spadoni, G.; Piersanti, G. An Improved Synthesis of *cis*-4-Phenyl-2-propionamidotetralin (4-P-PDOT): A Selective MT_2 Melatonin Receptor Antagonist. *Org. Biomol. Chem.* **2008**, *6*, 147−150.
(32) Wyrick, S. D.; Booth, R. G.; Myers, A. M.; Owens, C. E.; Kula, N. S.; Baldessarini, R. J.; McPhail, A. T.; Mailman, R. B. Synthesis and Pharmacological Evaluation of 1-Phenyl-3-amino-1,2,3,4-tetrahydronaphthalenes as Ligands for a Novel Receptor with Sigma-like Neuromodulatory Activity. *J. Med. Chem.* **1993**, *36*, 2542−2551.
(33) Copinga, S.; Tepper, P. G.; Grol, C. J.; Horn, A. S.; Dubocovich, M. L. 2-Amido-8-methoxytetralins: A Series of Nonindolic Melatonin-like Agents. *J. Med. Chem.* **1993**, *36*, 2891−2898.
(34) Bedini, A.; Spadoni, G.; Gatti, G.; Lucarini, S.; Tarzia, G.; Rivara, S.; Lorenzi, S.; Lodola, A.; Mor, M.; Lucini, V.; Pannacci, M.; Scaglione, F. Design and Synthesis of *N*-(3,3-Diphenylpropenyl)alkanamides as a Novel Class of High-Affinity MT_2-Selective Melatonin Receptor Ligands. *J. Med. Chem.* **2006**, *49*, 7393−7403.
(35) Garratt, P. J.; Vonhoff, S.; Rowe, S. J.; Sugden, D. Mapping the Melatonin Receptor. 2. Synthesis and Biological Activity of Indole Derived Melatonin Analogues with Restricted Conformations of the C-3 Amidoethane Side Chain. *Bioorg. Med. Chem.* **1994**, *4*, 1559−1564.
(36) Faust, R.; Garratt, P. J.; Jones, R.; Yeh, L. K.; Tsotinis, A.; Panoussopoulou, M.; Calogeropoulou, T.; Teh, M. T.; Sugden, D. Mapping the Melatonin Receptor. 6. Melatonin Agonists and Antagonists Derived from 6*H*-Isoindolo[2,1-*a*]indoles, 5,6-Dihydroindolo[2,1-*a*]isoquinolines, and 6,7-Dihydro-5*H*-benzo[*c*]azepino[2,1-*a*]indoles. *J. Med. Chem.* **2000**, *43*, 1050−1061.
(37) Wallez, V.; Durieux-Poissonnier, S.; Chavatte, P.; Boutin, J. A.; Audinot, V.; Nicolas, J. P.; Bennejean, C.; Delagrange, P.; Renard, P.; Lesieur, D. Synthesis and Structure−Affinity Activity Relationships of Novel Benzofuran Derivatives as MT_2 Melatonin Receptor Selective Ligands. *J. Med. Chem.* **2002**, *45*, 2788−2800.
(38) Fukatsu, K.; Uchikawa, O.; Kawada, M.; Yamano, T.; Yamashita, M.; Kato, K.; Hirai, K.; Hinuma, S.; Miyamoto, M.; Ohkawa, S. Synthesis of a Novel Series of Benzocycloalkene Derivatives as Melatonin Receptor Agonists. *J. Med. Chem.* **2002**, *45*, 4212−4221.
(39) Spadoni, G.; Balsamini, C.; Bedini, A.; Carey, A.; Diamantini, G.; Di Giacomo, B.; Tontini, A.; Tarzia, G.; Nonno, R.; Lucini, V.; Pannacci, M.; Stankov, B. M.; Fraschini, F. *N*-Acyl-5- and -2-5-Substituted Tryptamines: Synthesis, Activity and Affinity for Human MT_1 and MT_2 Melatonin Receptors. *Med. Chem. Res.* **1998**, *8*, 487−498.
(40) Rivara, S.; Mor, M.; Silva, C.; Zuliani, V.; Vacondio, F.; Spadoni, G.; Bedini, A.; Tarzia, G.; Lucini, V.; Pannacci, M.; Fraschini, F.; Plazzi, P. V. Three-Dimensional Quantitative Structure−Activity Relationship Studies on Selected MT_1 and MT_2 Melatonin Receptor Ligands: Requirements for Subtype Selectivity and Intrinsic Activity Modulation. *J. Med. Chem.* **2003**, *46*, 1429−1439.
(41) Jansen, J. M.; Copinga, S.; Gruppen, G.; Molinari, E. J.; Dubocovich, M. L.; Grol, C. J. The High Affinity Melationin Binding Site Probed with Conformationally Restricted Ligand-I. Pharmacophore and Minireceptor Models. *Bioorg. Med. Chem.* **1996**, *4*, 1321−1332.
(42) Cantor, S. E.; Tarbell., D. S. The Formation of *cis*- and *trans*-Perhydrobenzofurans from 2-(2-Methoxycyclohexyl)ethanol Derivatives. Reactions Proceeding through Methoxyl Participation. *J. Am. Chem. Soc.* **1964**, *86*, 2902−2909.
(43) Nonno, R.; Lucini, V.; Pannacci, M.; Mazzucchelli, C.; Angeloni, D.; Fraschini, F.; Stankov, B. M. Pharmacological Characterization of the Human Melatonin Mel_{1a} Receptor following Stable Transfection into NIH3T3 Cells. *Br. J. Pharmacol.* **1998**, *124*, 485−492.
(44) Bradford, M. M. A Rapid and Sensitive Method for the Quantitation of Microgram Quantities of Protein Utilizing the Principle of Protein−Dye Binding. *Anal. Biochem.* **1976**, *72*, 248−254.
(45) Cheng, Y. C.; Prusoff, W. H. Deoxyribonucleotide Metabolism in Herpes Simplex Virus Infected HeLa Cells. *Biochem. Pharmacol.* **1973**, *22*, 3099−3108.
(46) Spadoni, G.; Balsamini, C.; Bedini, A.; Diamantini, G.; Di Giacomo, B.; Tontini, A.; Tarzia, G.; Mor, M.; Plazzi, P. V.; Rivara, S.; Nonno, R.; Pannacci, M.; Lucini, V.; Fraschini, F.; Stankov, B. M. 2-[*N*-Acylamino(C1-C3)alkyl]indoles as MT_1 Melatonin Receptor Partial Agonists, Antagonists, and Putative Inverse Agonists. *J. Med. Chem.* **1998**, *41*, 3624−3634.
(47) *MacroModel*, version 9.7; Schrödinger, LLC: New York, NY, 2009.
(48) Allinger, N. L. Conformational Analysis. 130. MM2. A Hydrocarbon Force Field Utilizing V1 and V2 Torsional Terms. *J. Am. Chem. Soc.* **1977**, *99*, 8127−8134.
(49) Still, W. C.; Tempczyk, A.; Hawley, R. C.; Hendrickson, T. Semianalytical Treatment of Solvation for Molecular Mechanics and Dynamics. *J. Am. Chem. Soc.* **1990**, *112*, 6127−6129.
(50) Brunne, R. M.; van Gusteren, W. F.; Bruschweiler, R.; Ernst, R. R. Molecular Dynamics Simulation of the Proline Conformational Equilibrium and Dynamics in Antamanide Using the GROMOS Force Field. *J. Am. Chem. Soc.* **1993**, *115*, 4764−4768.
(51) Christianson, L. A.; Lucero, M. J.; Appella, D. H.; Klein, D. A.; Gellman, S. H. Improved Treatment of Cyclic β-Amino Acids and Successful Prediction of β-Peptide Secondary Structure Using a Modified Force Field: AMBER*C. *J. Comput. Chem.* **2000**, *21*, 763−773.
(52) Dolain, C.; Léger, J.-M.; Delsuc, N.; Gornitzka, H.; Huc, I. Probing Helix Propensity of Monomers within a Helical Oligomer. *Proc. Natl. Acad. Sci. U.S.A.* **2005**, *102*, 16146−16151.
(53) McDonald, D. Q.; Still, W. C. AMBER* Torsional Parameters for the Peptide Backbone. *Tetrahedron Lett.* **1992**, *33*, 7747−7750.
(54) Palocci, C.; Falconi, M.; Alcaro, S.; Tafi, A.; Puglisi, R.; Ortuso, F.; Botta, M.; Alberghina, L.; Cernia, E. An Approach To Address *Candida Rrugosa* Lipase Regioselectivity in the Acylation Reactions of Trytilated Glucosides. *J. Biotechnol.* **2007**, *128*, 908−918.
(55) Berl, V.; Huc, I.; Khoury, R. G.; Lehn, J.-M. Helical Molecular Programming: Folding of Oligopyridine-Dicarboxamides into Molecular Single Helices. *Chem.—Eur. J.* **2001**, *7*, 2798−2809.
(56) Berl, V.; Huc, I.; Khoury, R. G.; Lehn, J.-M. Helical Molecular Programming: Supramolecular Double Helices by Dimerization of Helical Oligopyridine-Dicarboxamide Strands. *Chem.—Eur. J.* **2001**, *7*, 2810−2820.
(57) *Maestro*, version 9.0, Schrödinger, LLC: New York, NY, 2009.
(58) Haasnoot, C. A. G.; de Leeuw, F. A. A. M.; Altona, C. The Relationship between Proton−Proton NMR Coupling Constants and Substituent Electronegativities—I: An Empirical Generalization of the Karplus Equation. *Tetrahedron* **1980**, *36*, 2783−2792.

■ NOTE ADDED AFTER ASAP PUBLICATION

After this paper was published online November 18, 2011, several minor corrections were made to the text. The corrected version was published November 28, 2011.